Beyond determinism: Accounting for weather variability in the carbon pricing debate for EU agriculture

Davit Stepanyan, Sebastian Neuenfeldt, Alisa Spiegel, Mareike Söder, Julio G Fournier Gabela, Florian Freund, Claudia Heidecke, Bernhard Osterburg, Alexander Gocht

European Review of Agricultural Economics, Vol **0** (**0**) (2026) pp. 1–33
https://doi.org/10.1093/erae/jbag007

Advance Access Publication 2 July 2026

Beyond determinism: Accounting for weather variability in the carbon pricing debate for EU agriculture

Davit Stepanyan [‡], Sebastian Neuenfeldt [‡], Alisa Spiegel[§], Mareike Söder[§], Julio G. Fournier Gabela[**], Florian Freund[**], Claudia Heidecke[§], Bernhard Osterburg[§], and Alexander Gocht[‡]

[‡]*Institute of Farm Economics, Johann Heinrich von Thuenen Institute, Braunschweig, Germany;* [§]*Coordination Unit Climate, Soil, Biodiversity Johann Heinrich von Thuenen Institute, Braunschweig, Germany;* [**]*Institute of Market Analysis, Johann Heinrich von Thuenen Institute, Braunschweig, Germany*

Received 19 June 2025; Final version accepted 26 March 2026

Abstract

Agriculture accounts for 11 per cent of EU greenhouse gas emissions, yet sectoral emissions have stagnated over the past two decades. This paper evaluates carbon pricing in EU agriculture by integrating stochastic yield variability into the CAPRI model. We assess how different carbon price levels affect emissions and outcome uncertainty. Results show that carbon pricing reduces emissions, and higher price levels are associated with lower uncertainty in policy outcomes. While expected results remain similar to deterministic simulations, stochastic modeling reveals greater regional and sectoral heterogeneity. These findings highlight the importance of accounting for production risk when designing agricultural climate policies.

Keywords: CAPRI model; carbon pricing; weather variability; stochastic modeling; EU agriculture

JEL classification: C63, Q18, Q51

1. Introduction

The European Union (EU) has committed to achieving carbon neutrality by 2050 and reducing its greenhouse gas (GHG) emissions by 55 per cent by 2030 relative to 1990 levels. Meeting these ambitious targets will require substantial mitigation efforts across all economic sectors, including agriculture (Frank

*Corresponding author: E-mail: davit.stepanyan@thuenen.de

et al., 2021). Although carbon pricing will apply to most sectors of the EU after 2030, the agriculture and land use, land use change and forestry sector remains exempt under the current EU policy framework. There are no provisions for its inclusion in carbon pricing from 2030 onwards; instead, mitigation efforts rely on non-pricing instruments and separate regulatory targets. In light of this, the European Scientific Advisory Board on Climate Change (ESABCC, 2024) strongly recommends implementing carbon pricing in EU agriculture as a cost-effective mitigation tool, capable of reducing GHG emissions through financial incentives and market-based price signals (World Bank, 2021). Denmark is leading the way in this regard, becoming the first country to implement a national carbon pricing scheme specifically targeting agricultural emissions (Sørensen *et al.*, 2025). Given these developments, it is crucial to understand how carbon pricing may affect agricultural production, incomes and the spatial distribution of GHG emissions across EU countries.

Several studies have investigated the impact of carbon pricing on EU agriculture under deterministic settings (Himics *et al.*, 2018, 2020; Frank *et al.*, 2021; Stepanyan *et al.*, 2023). However, agricultural GHG emissions are highly sensitive to yield outcomes, which in turn are largely determined by weather variability. As a result, it remains unclear how weather-induced yield fluctuations[1] may influence the environmental and socio-economic impacts of carbon pricing in agriculture. This study addresses this knowledge gap by integrating yield variability into the Common Agricultural Policy Regionalized Impact (CAPRI) model to simulate the introduction of a carbon price in the EU agricultural sector.

Agriculture accounts for approximately 11 per cent of total GHG emissions in the EU, making it the second-largest source after the energy sector, which contributes around 77 per cent (EEA, 2021). The bulk of agricultural emissions comes from methane (CH_4) and nitrous oxide (N_2O), primarily due to livestock, manure management and fertilizer use (Fellmann *et al.*, 2018). Prior research has consistently found that the livestock sector is particularly vulnerable to carbon pricing, with key impacts observed in terms of carbon leakage and changes in farm income resulting from shifts in output prices. For example, Frank *et al.* (2021) found that at a carbon price of USD 245 per ton of CO_2 equivalent (tCO_2eq), approximately 40 per cent of the emissions mitigated within the EU are offset by increases outside the EU, although global net emissions still decline. Himics *et al.* (2018) reported a 21 per cent leakage rate at a price of €50/tCO_2eq, which increases to 50 per cent when combined with trade liberalization, yet still results in net global mitigation. Himics *et al.* (2020) found a 20 per cent leakage rate under a non-uniform carbon pricing scheme. Across all studies, the livestock sector emerges as the most affected by agricultural carbon pricing. Stepanyan *et al.* (2023) further showed that the inclusion of technical mitigation options can significantly reduce the estimated leakage rates.

1 While yield deviations may reflect factors beyond weather, such as pests or management decisions, at the annual national scale considered here weather variability is widely recognized as the dominant driver of yield fluctuations. Accordingly, the stochastic component is interpreted as capturing weather-dominated production risk.

Unlike other sectors, agricultural productivity is highly dependent on weather conditions. Years characterized by extreme droughts and heatwaves, such as 2003 and 2018, resulted in substantial yield reductions across various EU regions (Ciais *et al.*, 2005; BMEL, 2018; Webber *et al.*, 2020). Because annual yield variability directly affects GHG emissions, it is plausible that the socio-economic and environmental impacts of carbon pricing are also influenced by such variability. To our knowledge, no previous study has explicitly incorporated stochastic yield shocks when assessing the effects of GHG mitigation policies in the agricultural sector.

To address this gap, we

1. introduce an uncertainty quantification module into the CAPRI model by integrating stochastic elements;
2. analyze how weather-induced yield uncertainty modifies the effects of carbon pricing in the EU agricultural sector; and
3. simulate different carbon price levels to assess the robustness of results across different pricing scenarios.

The paper's structure is as follows: Section 1.1 provides an overview of stochastic simulation modeling. Section 2 describes the CAPRI model, the methodological framework employed and the data sources used for generating stochastic components. Section 3 outlines the policy scenarios simulated. Section 4 presents and interprets the simulation results. Finally, Section 5 discusses the findings and concludes with key policy implications.

1.1 Stochastic simulation modeling

In recent decades, advances in computational power and processing speed have enabled simulation models, particularly those addressing agricultural and environmental issues, to evolve significantly in both scope and complexity. However, this increasing complexity has also raised concerns about the inherent uncertainty in model outputs. Reflecting these concerns, the manifesto for good modeling practices, by Saltelli *et al.* (2020), underscores the importance of integrating uncertainty quantification into simulation-based analyses.

Incorporating stochastic elements into simulation models can enhance the richness and policy relevance of the results in several ways:

(a) **Identification of critical variables:** It identifies model variables or parameters that are most sensitive to a specific source of uncertainty. This insight is valuable during model development and in policy evaluation, particularly when assessing the risks associated with different policy options.

(b) **Probabilistic outcome ranges:** Stochastic models generate distributions of potential outcomes rather than single-point estimates. This allows for a more nuanced understanding of how uncertain inputs, such as weather conditions, market prices or consumer demand, translate into variability in model outputs.

(c) **Threshold analysis:** Stochastic modeling enables estimation of the probability that specific thresholds will be crossed within a given time frame. For example, it can assess the likelihood that tariff rate quotas will be fully utilized or the probability that a policy will significantly affect farm income.
(d) **Joint event scenarios:** It facilitates the formulation of scenarios in which multiple uncertain events occur simultaneously. For instance, the model can assess the combined impact of low crop yields and high oil prices, accounting for the spatial and temporal correlations between these phenomena.

Numerous studies emphasize the limitations of deterministic models in capturing dynamics that are better represented stochastically. For example, Westhoff *et al.* (2006) show that while deterministic projections fail to predict that the USA will exceed the World Trade Organization producer support threshold, a stochastic analysis estimates a 42 per cent likelihood of this outcome. Similarly, Glauber and Westhoff (2015) find that deterministic projections of US Farm Bill costs underestimate fiscal uncertainty by up to USD 5 billion. Meyer *et al.* (2012) argue that deterministic models fail to adequately capture the market effects of biofuel policies, potentially underestimating technology adoption. Using a stochastic general equilibrium framework, Arndt and Hertel (1997) challenge Batra's (1992) conclusion that technological progress in Japan explains declining US real wages, instead suggesting that wage increases in the USA are equally likely. Chatzopoulos *et al.* (2021) employ stochastic simulation using multivariate copulas to model concurrent and recurrent climate extremes, finding that extreme agro-climatic anomalies significantly distort the global agricultural market equilibrium and that trade and storage serve as important alleviative mechanisms for market uncertainty. Record-high global commodity prices can result from either single-country extremes or simultaneous events across multiple regions.

To address such uncertainties, researchers increasingly apply uncertainty quantification methods through stochastic modeling, which is now considered standard practice in many modeling frameworks (Stepanyan *et al.*, 2021). In this context, "stochastic" refers to models in which key parameters are not fixed but are drawn from defined probability distributions, enabling simulations to reflect the range and likelihood of real-world outcomes.

2. Methodology and data

2.1 The CAPRI modeling system

The CAPRI[2] model is a global, comparative-static, partial-equilibrium (PE) model for the agricultural sector, designed for policy impact assessment of the Common Agricultural Policy (CAP) and trade policies (Gocht and Witzke,

2 Model revision number: 10001; date of release: 25 January 2022. For more details about the model, please refer to Online Appendix 3.

2024). CAPRI consists of two major modules: (1) a highly detailed and disaggregated supply module for the European agricultural sector and (2) a global market module. These two modules are linked via a sequential calibration approach that provides price feedback to simulated policy shocks.

The supply module comprises independent non-linear programming models for each of the 280 NUTS 2 regions of the EU 27, Norway, the Western Balkans and Turkey, representing approximately fifty animal and crop activities. The individual supply models are based on the Positive Mathematical Programming approach, which provides a high degree of flexibility for capturing meaningful interactions between production activities and the environment (Gocht *et al.*, 2017). Each supply model maximizes the regional agricultural income subject to land constraints, nutrient balances and policy requirements. These individual models also include low- and high-intensity variants for different production activities, while a non-linear cost function captures the effects of labor and capital on farmers' decisions (Gocht and Witzke, 2024).

The market module is a comparative-static, deterministic, spatial and global PE model that depicts approximately sixty primary and secondary agricultural products. It represents eighty countries or country blocks worldwide. International trade is modeled using the Armington assumption, whereby goods are differentiated by place of origin according to consumer preferences derived from historical trade patterns. This approach allows modeling bilateral trade flows between countries as well as various bilateral and multilateral trade instruments (Gocht and Witzke, 2024).

Market equilibrium in CAPRI is reached through iterative interactions between the supply and market modules. During the iterative interaction, the supply module is first solved under fixed prices, and the resulting supply and feed-demand changes are used to shock the supply and feed-demand modules of CAPRI at the country level in the EU. After solving the market module, the new prices for the EU regions are delivered to the regional supply modules. These iterations between the two modules continue until convergence is reached. Therefore, we describe this as an iterative approach, in which we solve the 270 regional mathematical supply models and the PE market model in consecutive steps.

A key aspect of CAPRI relevant to this study is its modeling of crop yields. In a non-stochastic setting, the yield response is driven by three distinct structural mechanisms. First, the regional composition effect accounts for spatial reallocation. This mechanism tracks changes in the weights of various geographic units, illustrating how aggregate yields are affected when the locus of production shifts between regions with disparate baseline productivities, such as between Member States or across the broader EU. Second, the technology mix included in CAPRI's supply models' mathematical programming models reflects internal substitution among production systems. This involves shifts in the relative shares of low- and high-yield variants within a specific crop and region, representing a transition across different technological frontiers rather than a movement along a single production function. Finally, endogenous intensification—or the yield elasticity effect—captures adjustments to input–

output coefficients within specific technologies. This process is governed by iso-elastic yield functions, which model how producers calibrate management intensity in a direct response to output price fluctuations. The iterative framework of the CAPRI model facilitates a dynamic updating of supply model parameters. Market-level price signals are integrated back into the supply models, and subsequently, yield and input coefficients are updated. The yields (Y) of different agricultural activities (j) in the model adjust endogenously during the iterative process, reacting via an iso-elastic function to changes in producer prices (p_o):

$$\log\left(Y_j\right) = \alpha_j + \varepsilon_j \log\left(p_o\right), \tag{1}$$

where ε features yield elasticities and α is the intercept.

Given the iterative solution process of CAPRI, and to spare the necessity of calculating the constant term α, equation (1) has been rearranged by taking the ratio of yields in two consecutive iterations:

$$\frac{Y_{j,t}}{Y_{j,t-1}} = \left(\frac{p_{o,t}}{p_{o,t-1}}\right)^{\varepsilon_j}. \tag{1.1}$$

Finally, by rearranging equation (1.1), price-dependent yields are calculated as follows:

$$Y_{j,t} = Y_{j,t-1}\exp\left(\varepsilon_j \log\frac{p_{o,t}}{p_{o,t-1}}\right). \tag{1.2}$$

The yield elasticities with respect to producer prices are taken from the estimated elasticities from the Aglink-Cosimo model (OECD/FAO, 2015). For details on the estimation of these elasticities, please refer to Jongeneel and Gonzalez-Martinez (2020). These elasticities are available at the country level for the major arable crops, and range from 0.2 to 0.3.

CAPRI has been frequently used for ex-ante assessment of agricultural, environmental and trade policies. For example, in recent years, CAPRI has been frequently employed to assess different climate change mitigation policies on a global (e.g. Hasegawa *et al.*, 2018; van Meijl *et al.*, 2018; Frank *et al.*, 2019, 2021) and regional (e.g. Fellmann *et al.*, 2018; Himics *et al.*, 2018, 2020; Jansson and Säll, 2018) scale. CAPRI is also often used to analyze questions related to the CAP. In this context, Gocht *et al.* (2017) examine the economic and environmental impacts of CAP greening measures, and Jansson *et al.* (2020) analyze the impacts of reallocating Voluntary Coupled Support payments to the Basic Payment Scheme.

CAPRI endogenously accounts for CO_2 and non-CO_2 emissions and removals in the EU agricultural sector based on a detailed nutrient flow model per activity in each region, following the IPPC guidelines (IPCC, 2006). It accounts for approximately 98.4 per cent of the total EU agricultural GHG emissions officially reported to the UNFCCC (Table 1). Tier 2 approach of the IPCC guidelines is mainly used in CAPRI; however, in cases when the necessary data are missing, the Tier 1 approach is used (e.g. rice cultivation). Detailed descriptions of the methods used to calculate agricultural emission invento-

Table 1. GHG emission sources accounted for by CAPRI.

Emissions	Sources modeled in CAPRI
CH_4	■ Enteric fermentation ■ Manure management ■ Rice cultivation
N_2O	■ Synthetic fertilizer ■ Manure management (application) ■ Excretion on pasture ■ Crop residues ■ Histosols ■ Deposition of ammonia ■ Emissions due to leaching of nitrogen
CO_2	■ Liming

Source: Pérez Domínguez et al. (2020) .

ries in regional supply models can be found in Pérez Domínguez (2005), Leip *et al.* (2010) and Pérez Domínguez *et al.* (2016). Since this approach covers only GHG emissions in the EU, a complementary GHG emissions accounting for the rest of the world is implemented in the market module to measure emission leakage. In the market module, GHG emissions are computed using the emission intensities (EIs) of agricultural commodities. Detailed information on the estimation of EI is provided in Jansson and Säll (2018).

2.2 Estimating weather-induced yield variability

Agricultural production, and crop yields in particular, exhibit substantial year-to-year volatility, primarily due to weather variability (Burrell and Nii-Naate, 2013). For example, Fig. 1 presents the coefficient of variation (CV) of wheat yields in the EU from 1961 to 2020. The data clearly indicate that wheat production is subject to considerable annual and regional fluctuations. However, these dynamics are not adequately captured by traditional deterministic simulation models, which are typically calibrated using average yields. To address this limitation, we have incorporated stochastic yield variables into the CAPRI model.

To reduce model dimensionality, important crop-producing activities across twenty-four countries, measured by production levels, have been selected for stochastic modeling. This yielded 253 country-crop combinations.[3] Country-level data for the period of 1995–2017 are used to generate the stochastic components. Burrell and Nii-Naate (2013) suggest calculating these

3 Countries with insignificant activity levels have not been selected. This selection led to the following group of countries with stochastic yields: Austria, Bulgaria, Belgium, Cyprus, Czech Republic, Germany, Denmark, Estonia, Greece, Spain, Finland, France, Hungary, Ireland, Italy, Lithuania, Latvia, the Netherlands, Poland, Portugal, Romania, Sweden, Slovenia and the Slovak Republic.

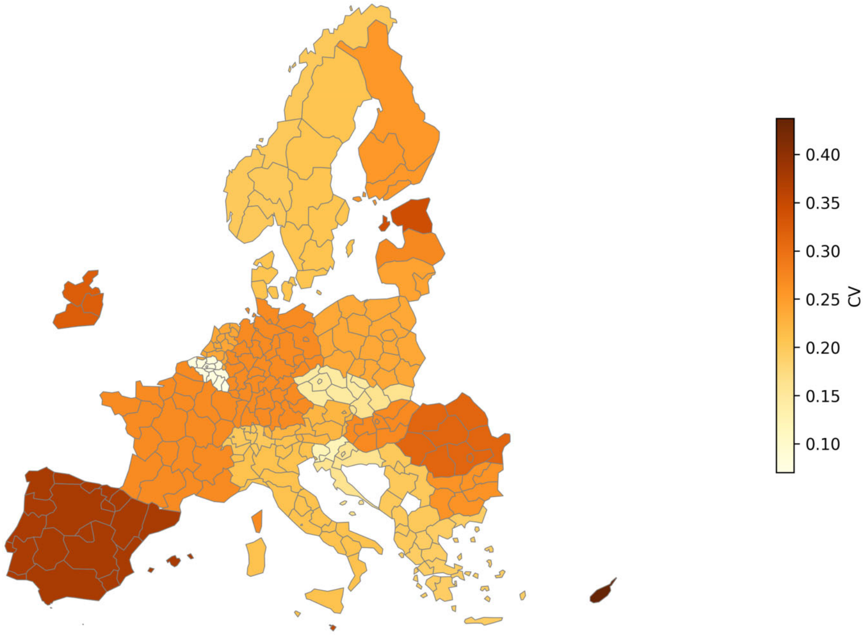

Fig. 1. Coefficient of variation (CV) of historical wheat yields in the EU 27, 1961–2020. *Source*: FAOSTAT (2022).

stochastic components ($Z_{c,t}$) for variable $c = (1, 2,..., n)$, in the year $t = (1, 2,..., m)$ as deviates from estimated linear trends ($\hat{y}_{c,t}$), that is

$$Z_{c,t} = \frac{y_{c,t}}{\widehat{y_{c,t}}} - 1, \tag{2}$$

where $y_{c,t}$ is the observed yield of crop c in the year t.

Araujo-Enciso *et al.* (2017) show that capturing the stochastic yield components as deviates from estimated cubic trends yields more reliable results[4] as measured by the mean squared error between the fitted values and the true historical values. Thus, we follow the latter approach and generate de-trended yield deviations for each stochastic crop–country combination. Normality was empirically assessed using the Shapiro–Wilk test, and crop–country combinations for which the null hypothesis of normality was rejected, and which contributed negligibly to aggregate production, were excluded from the stochastic analysis to avoid introducing noise. For a small number of relevant cases where normality was initially rejected, alternative trend specifications were applied to obtain normally distributed deviations and preserve spatial coherence. The resulting stochastic system represents the vast majority of EU production (Table A1, Appendix 1). This approach enables the use of the Informed Rotations of Gaussian Quadratures (IRGQ) method (Stepanyan *et al.*,

4 Araujo-Enciso *et al.* (2017) used the Clayton copula approach to generate the empirical cumulative distribution function for yields.

2022) (explained in Appendix 2) to efficiently reproduce the second central moments of a high-dimensional joint distribution.

Based on these deviates, a covariance matrix (Σ) is constructed to capture the inter- and intra-regional correlations of crop yields in the EU. The covariance matrix is then used to generate a multivariate normal distribution of yield variables, from which the stochastic variables are drawn using the IRGQ method described in Appendix 2. As noted in Section 2.2, there are 253 stochastic yield variables identified in the model. Since the applied method requires only $2n$ stochastic points to approximate the probability distribution, we end up with 506 vectors of stochastic shocks per crop applied iteratively in the model. Following the above-described approach, we obtain normally distributed stochastic shocks for each yield variable, with mean 0 and standard deviation ranging from 0 to 1.

2.3 Solution to the problem in the stochastic settings

Solving simulation problems while considering uncertainties is not new, and various approaches have been implemented in different models. For example, the AGLINK-COSIMO model, which is a well-known PE model used to study global agricultural markets, applies the Latin hypercube sampling method for stochastic analysis (OECD/FAO, 2015; Chatzopoulos *et al.*, 2021). The GLOBIOM model, which is also a widely used global PE model to analyze the competition for land between agricultural, forestry and bioenergy sectors, applies the Monte-Carlo method (Fuss *et al.*, 2015; Valin *et al.*, 2015; Ermolieva *et al.*, 2016). The GTAP model has a long history of applying the Gaussian Quadratures (GQ) approach as an efficient method for quantifying both parametric and shock uncertainty, beginning with the pioneering work of Arndt (1996) and subsequently extended through a wide range of methodological developments and policy analyses (Valenzuela *et al.*, 2007; Verma *et al.*, 2011; Lobell *et al.*, 2013; Villoria *et al.*, 2013; Villoria and Mghenyi, 2017). Stepanyan *et al.* (2021) provide an overview of different stochastic modeling methods.

We employ the IRGQ method proposed by Stepanyan *et al.* (2022) to generate yield realizations and their corresponding weights that mimic the underlying yield distribution (see Appendix 2 for further details). The model is solved for each yield draw, outputting a vector of outcomes and a weight assigned to the corresponding yield realization (Fig. 2). These vectors are used to reconstruct resulting distributions for each outcome variable. The associated code is integrated into the CAPRI model and openly available for use.[5]

With the IRGQ, we enable stochastic simulation for models with complex iterative solving algorithms, such as the CAPRI model,[6] which depicts the intricate interactions between farms and agricultural policies within global mar-

5 To access the latest stable release of the CAPRI model, visit www.capri-model.org.

6 CAPRI's computational complexity arises not only from the size of the underlying non-linear system, but primarily from the iterative procedure required to establish market equilibrium. Each simulation involves repeatedly solving the global market model together with approximately 270 regional supply models until convergence is achieved. The number of iterations, and thus the computational burden, increases with the magnitude and non-linearity of the implemented shock.

		Deterministic settings *(no yields variability)*	**Stochastic settings** *(yields variability in the form of standard deviation from estimated historical trend)*
Reference scenario	No policy	We focus on deterministic outcomes for 1. Optimal production activities 2. Optimal sources and resulting remains of nitrate used 3. Agricultural income 4. Agricultural emission, incl. leakage	Annual yield realisations (n=506) are drawn independently from a multivariate normal distribution ↓ The IRGQ method is used to draw yields realisations and their weights to mimic the underlying distribution of yields ↓ The model is solved for each yields realisation outputting a vector of outcomes and a weight assigned to the corresponding yields realisation ↓ A set of outcomes and weights is used to reconstruct resulting distributions for 1. Optimal production activities 2. Optimal sources and resulting remains of nitrate used 3. Agricultural income 4. Agricultural emission, incl. leakage
Policy scenario	Future value of the emission tax is extracted from agricultural income in the supply model: $-ET * (1+i)^t * (Em - \overline{Em})$ Where ET stays for emissions tax; i stays for annual interest rate; Em stays for agricultural emissions; and $\overline{Em}$ stays for allocated emissions permits. Two levels of emissions tax are considered: 50€/CO_{2eq} (CP50) and 100€/CO_{2eq} (CP100)		

Fig. 2. Schematic representation of scenarios and the solution method under deterministic and stochastic settings. *Source*: own elaboration.

Scenario	**Type**	**Process Flow**	**Key Assumptions**	**Comparison Basis**
Reference	***Deterministic***	[Business as Usual]	No policy shocks; Deterministic trends	–
CP50	***Deterministic***	[ ] → [Adjust] → [Emissions]	Farmers are flexible to adjust activity and input levels	CP50 vs. Reference
CP100	***Deterministic***	[ ] → [Adjust] → [Emissions]	Farmers are flexible to adjust activity and input levels	CP100 vs. Reference
CP50 +	***Stochastic***	[CP50] →[ ]+ [ ] → [Distributions]	Activity/input levels fixed to CP50; stochastic yield shocks applied.	CP50 + vs. Reference
CP100 +	***Stochastic***	[CP100] →[ ] + [ ] → [Distributions]	Activity/input levels fixed to CP100; stochastic yield shocks applied.	CP100 + vs. Reference

Fig. 3. Simulated scenarios' design workflow (carbon price: ; uncertainty: ; fixed: ; business as usual: ; reference: ; activity/input levels: ; distributions of results:).

kets, thereby enabling stochastic analyses in a regionalized context, as presented in this paper. For the first time, we can model yield variability and the intricate interactions between markets. Earlier approaches required high repetitions of scenario simulations, which were only possible for models with a higher degree of abstraction.

3. Policy design and assessment

All simulated scenarios are presented in Fig. 3. The reference scenario serves as a baseline for comparison with the counterfactual scenarios described below, focusing on projections for variables in the year 2030. It represents a business-as-usual case, reflecting anticipated developments in the agricultural sector and policy changes foreseen under existing legislation. This scenario is calibrated to align with the European Commission's agricultural outlook and incorporates trends in technological progress, such as yield growth and improvements in feed and fertilizer efficiency, as well as broader economic indicators, including inflation, GDP growth and population change. The simulated policy scenarios build upon the reference scenario by incorporating additional shocks specific to each case.

In particular, the reference scenario without a carbon price is compared with two carbon pricing scenarios: a moderate carbon price of €50 per ton of CO_2-equivalent (CP50) and a higher carbon price of €100 per ton (CP100). These levels represent the lower and upper bounds of carbon price fluctuations observed in the EU Emissions Trading System in 2022.

The transmission of carbon price shocks into the model is implemented as follows: first, the future value of the carbon price is determined using an assumed annual interest rate of 1.9 per cent. Second, it is assumed that the carbon price is levied only on emissions exceeding a benchmark level, defined as the emissions recorded under the reference scenario (i.e. emission permits). The resulting real value of the carbon price is subtracted from agricultural income in the supply module. This adjustment is reflected in the objective function of the supply models as follows:

$$-ET * (1+i)^t * \left(Em - \overline{EM}\right), \tag{3}$$

where ET is the designated carbon price,[7] i is the annual interest rate, Em is the actual total agricultural emissions in CO_2eq accounted for in the model and $\overline{Em}$ stays for the allocated emission permits at the regional level. It is worth noting the presence of a negative sign in front of the expression, which means that it is incorporated into the objective (profit maximization) function as a cost. However, as only emissions exceeding the allotted emission permits are priced, this cost can be considered a subsidy in the case of a reduction in emissions.

Given that the carbon price scenarios are designed as long-term shocks, it is assumed that farmers have full flexibility to adapt their production systems accordingly. In CAPRI, producer behavior is governed by profit maximization, with carbon costs entering the profit function as additional production costs. This allows farmers to respond by adjusting activity levels,[8] for example, by shifting away from more emission-intensive activities, by extensifying production or by changing input use. In livestock production, this includes adjustments in the feed mix, which responds to changes in relative prices given the pre-defined needs of each animal category. Feed rations in CAPRI consist of tradable feed items, including industrial feed, as well as non-tradable components such as fodder, straw and on-farm milk used for feeding.

Since the environmental and economic impacts of the carbon price scenarios are directly influenced by weather-related uncertainty, we also account for

7 The calculated future (discounted) values corresponding to the considered carbon prices are as follows: 50€/tCO_2eq $\rightarrow$ 60.35€/tCO_2eq, 100€/tCO_2eq $\rightarrow$ 120.71€/tCO_2eq.

8 In this context, activity level refers to the level of production measured in heads of livestock or hectares of land.

this source of variability as it is transmitted to the model through crop yields. Weather-driven yield variability represents a short-term shock that typically occurs after farmers have already incurred costs for fertilization and plant protection. As a result, input and production decisions must be made under uncertainty, based on historical experiences and expectations about future yields. Weather shocks, such as droughts or extreme heat, usually occur during critical phenological stages, at which point farmers are no longer able to adjust their production plans.

Weather variability is explicitly modeled for EU crop yields only, reflecting the detailed representation of agricultural production within the EU in CAPRI, while production outside the EU is represented in a more aggregated manner on the market side. Consequently, the analysis focuses on how EU agricultural production, emissions and market outcomes respond to domestic weather uncertainty. The results should therefore be interpreted as conditional on EU weather variability and do not capture the full transmission of weather shocks originating in non-EU producing regions.

In contrast, a carbon price constitutes a long-term shock, allowing farmers to respond by modifying their production systems. To quantify the effects of both types of shocks in the CAPRI model, we employ a two-stage approach following the methodology proposed by Ermolieva *et al.* (2016) and Britz (2022), which assumes non-state-contingent production. This approach is operationalized in the following steps:

1. First, the reference scenario is simulated under deterministic conditions.
2. Next, the carbon price scenarios are simulated under the assumption that farmers are fully flexible and can adjust their production systems accordingly.
3. In the third step, we fix the activity levels, as well as fertilizer and other input costs, at the levels determined in the second step. On top of these fixed values, we apply stochastic yield shocks, that is we run the model for each carbon price scenario 506 times, reflecting the 506 vectors of randomly drawn yield shocks. As discussed above, this step assumes that farmers cannot anticipate weather-related shocks and therefore cannot adapt their production patterns in advance.

For animal production activities, we allow for minor adjustments in activity levels (±1 per cent), acknowledging that farmers may decide to slaughter animals earlier or delay based on feed availability and feed prices. At this stage, endogenous yield responses are not permitted, consistent with the assumption outlined in equation (1). Since the demand for fodder maize used in biofuel production is exogenous in the model, we assume that stochastic yield shocks shift the corresponding demand curve accordingly. Grass silage is not modeled stochastically, as farmers can buffer yield fluctuations through on-farm stock adjustments, which are not explicitly represented in the model.

This third step generates stochastic outcomes for the respective policy scenario. The effects of the policy under yield uncertainty are then evaluated by comparing the stochastic results with those of the reference scenario.

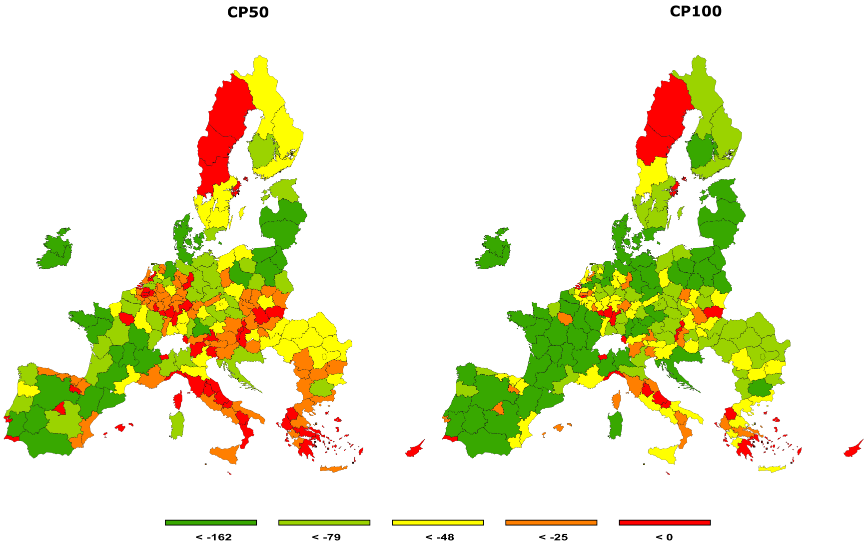

Fig. 4. Mitigated emissions in 1000t CO_2eq compared to the reference scenario, in absolute terms.

4. Results

The following two subsections present the results of the simulated scenarios compared to the baseline in 2030 under the deterministic and stochastic model setups. First, we describe the results without yield uncertainty (deterministic). This helps to understand how the model reacts to the simulated shocks without stochastic yield elements, thus making it easier to grasp the results under yield uncertainty, which adds an additional layer of complexity to the model. In the second subsection, we describe the results under the stochastic model setup.

4.1 Carbon price without yield uncertainty

The implementation of the 50€/tCO_2eq and 100€/tCO_2eq carbon price scenarios without considering yield uncertainty reduces the EU agricultural emissions by 17.2MtCO_2eq (4.5 per cent) and 33MtCO_2eq (8.6 per cent), respectively, compared to the reference scenario in 2030. These positive environmental effects are mainly due to production reallocation from the EU to more competitive non-EU countries, which leads to substituting domestic production in the EU with imports.

Given that the livestock sector is more emission-intensive than the crop sector, it is more strongly affected by the EU carbon pricing scenarios. As a result, the majority of the achieved emissions reduction in the EU, around 69 per cent, is attributed to the livestock sector, while the abatement in the crop sector is comparatively smaller at 31 per cent in both scenarios. This is also evident in Fig. 4, where most mitigation occurs in predominantly animal-producing regions, such as France, Ireland, Germany and Spain. Regional differences in emission reductions are substantial, ranging from almost no

Table 2. Summary of the results. *Source*: own elaboration.

			CP50		CP100	
			Results are presented compared to the baseline in 2030			
Topic	Indicator	Unit	EU	Non-EU	EU	Non-EU
	Agricultural GHG emission	$MtCO_2eq$ (per cent)	−17.2 (−4.5)	+12.1 (0.14)	−33 (−8.6)	17.5 (0.24)
Area	Agricultural area	million.	−1	–	−2.08	–
	Set-aside and fallow	hectares	+1	–	+1.9	–
Beef	EU production	Per cent	−5	0.17	−9.80	0.27
	Exp. share world		−1.3	1.30	−2.12	2.12
	Imp. share world		0.01	−0.01	−0.02	0.02
Pork	EU production	Per cent	−2.08	0.43	−4.05	0.78
	Exp. share world		−3.85	3.85	−7.05	7.05
	Imp. share world		0.36	−0.36	0.36	−0.36
Sheep and goat meat	Productions EU	Per cent	−5.11	0.08	−9.96	0.14
	Exp. share world		−1.42	1.42	−2.72	2.72
	Imp. share world		1.03	−1.03	1.76	−1.76
Poultry	EU production	Per cent	−0.27	0.04	−0.51	0.07
	Exp. share world		−0.56	0.56	−1.05	1.05
	Imp. share world		0.22	−0.22	0.39	−0.39
Cereal	EU production	Per cent	−2.08	0.07	−4.12	0.17
	Exp. share world		−0.76	0.76	−1.56	1.56
	Imp. share world		−0.19	0.19	−0.19	0.19
Oilseed	EU production	Per cent	−1.36	0.05	−2.70	0.14
	Exp. share world		−0.21	0.21	−0.41	0.41
	Imp. share world		−0.05	0.05	−0.04	0.04
N-balance	Input mineral N	Per cent	−5.23	–	−9.78	–
	Input manure N		−3.70	–	−6.84	–
	Surplus		−4.88	–	−9.49	–
	Surplus at soil		−8.95	–	−14.22	–
Income	Consumer surplus	€ bn	−7.60(−0.05)	−9(−0.01)	−15.6(−0.1)	−17.3(−0.02)
	Agri. factor income	(Per cent)	9.9(8.25)	−25.8(−7.0)	19.9(16.5)	−25.1(−7.1)

Note: If the model does not cover a particular indicator, a dash (–) is shown in its place.

change (Praha, Czech Republic) to 1.2$MtCO_2eq$ in the Southern and Eastern regions of Ireland.

The CP50 and CP100 scenarios result in a decline of the utilized agricultural area (UAA) in the EU by 1 million ha (0.63 per cent) and 2.08 million ha (1.3 per cent), respectively, while set-aside and fallow land increase by 1 million ha (10.86 per cent) and 1.9 million ha (20.04 per cent), respectively. Furthermore, the size of the beef cattle herd in the EU decreases by 9.7 and 18.5 per cent, respectively, leading to a reduction in beef production by 5 and 9.8 per cent (Table 2). Similarly, the number of animals in pork production decreased by 2.08 per cent (4.05 per cent), and in sheep and goat meat production the number decreased by 5.11 per cent (9.96 per cent), under the CP50 (CP100) scenario (Appendix 1, Fig. A1). Conversely, changes in poultry meat production are not significant. Cereal production decreases by 2 and 4.1 per cent following a reduction in the UAA devoted to cereals by 1.7 and 3.4 per cent under the CP50 and CP100 scenarios, respectively.

When examining changes in beef cattle herd sizes at the NUTS 2 level, significant reductions are evident, primarily in regions known for substantial beef production (Appendix 1, Fig. A2). The most notable reductions occur in Irish regions, Portugal (Alentejo), Spain (Castilla-Leon, Extremadura) and France (Auvergne, Bourgogne, Midi-Pyrenees, Limousine and Pays de la Loire).

Following the production changes in the EU agricultural sector, a reduction of fertilizer input with mineral fertilizers, manure and crop residues is observed (Appendix 1, Table A2). Due to a decrease in production levels of fodder on arable land as well as in intensive grassland areas, the biological fixation of nitrogen drops by 4.95 and 9.55 per cent under CP50 and CP100 scenarios, respectively. Declined crop production drives down the absorption (export of nutrients) by crops. Therefore, the total surplus of nitrate drops by 4.88 and 9.49 per cent under CP50 and CP100 scenarios, respectively.

As is well known in the literature, a unilateral carbon price policy in the EU could lead to emissions shifting to other regions, resulting in the leakage effect (Frank *et al.*, 2021). Emission leakage is detrimental as it reduces the effectiveness of unilateral climate policies while imposing economic costs on domestic farmers. In Table 2, we observe that the simulated scenarios result in considerable leakage. More precisely, under the CP50 scenario, around 12 $MtCO_2eq$ (71 per cent) of the EU mitigation effort is leaked to non-EU countries, resulting in a net decrease in global agricultural emissions by about 5 $MtCO_2eq$ (0.09 per cent). Under the CP100 scenario, about 17.5 $MtCO_2eq$ (53 per cent) of the EU mitigation effort is leaked to non-EU countries, resulting in a net decrease in global agricultural emissions by 15 $MtCO_2eq$ (0.27 per cent). This shows that the relationship between carbon price levels and leakage is not linear but rather logarithmic, that is increasing at a decreasing rate.

Considering that the livestock sector in the EU is responsible for most of the GHG abatement, it is also important to investigate the leakage effect directly caused by this sector. The reallocation of beef production alone is responsible for 24 per cent (21 per cent) of the leaked GHG emissions from the EU under the CP50 (CP100) scenario. Most of the leakage is observed in India, Mercosur countries, Africa, China and North America (Appendix 1, Fig. A3). The leakage effect due to the reallocation of pork production is more modest as it is less emission-intensive. This sector is responsible for 3.4 per cent (3.5 per cent) of the leaked GHG emissions from the EU under the CP50 (CP100) scenario. The reallocation of pork production primarily results in leakage in North America, Mercosur countries and China (Appendix 1, Fig. A4).

The observed leakage occurs mainly through the competitiveness channel.[9] The human consumption of beef in the EU has reduced by 3 per cent (6.2 per cent) under the CP50 (CP100) as a result of increased prices by 12 per cent (26 per cent). The beef prices in the rest of the world also increase slightly, that is 0.4 and 0.8 per cent, leading to a reduction in demand by 0.03 and 0.05 per cent under the CP50 and CP100 scenarios, respectively. As the EU reduces

9 Two leakage channels are differentiated in literature: competitiveness and international price channels (Böhringer *et al.*, 2012). Under the competitiveness channel (producer-side), domestic producers lose competitiveness due to higher costs. Thus, the domestic production is being replaced by imports. Under the international price channel (market-side), assuming that the regulating country is a price setter, the demand in the regulating country shrinks causing reduction in international prices, which increases the demand in the rest of the world.

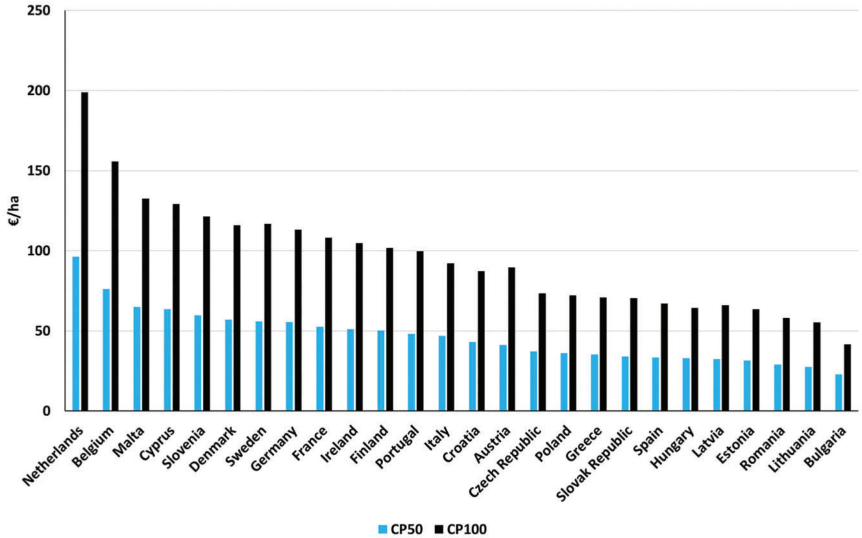

Fig. 5. Absolute change in agricultural income per member state compared to the reference scenario in 2030.

its share of global beef exports by 1.30 per cent under the CP50 scenario (2.12 per cent under CP100) and increases its share of global beef imports by 0.01 per cent under CP50 (while decreasing it by 0.02 per cent under CP100), some countries expand their production to meet the unmet demand in the global market (Table 2). By contrast, the reallocation of cereal and oilseed production results in only 5.5 per cent of the emissions mitigated in the EU being leaked to non-EU countries under CP50 (3.6 per cent under CP100) and 1.1 per cent under CP50 (0.8 per cent under CP100), respectively.

The introduction of carbon pricing in the EU increases agricultural commodity prices, thereby reducing consumer surplus. Under the CP50 and CP100 scenarios, consumer surplus declines by €7.6 billion (−0.05 per cent) and €15.6 billion (−0.1 per cent), respectively. Conversely, agricultural income in the EU rises by €9.9 billion (8.25 per cent) under CP50 and by €19.9 billion (16.52 per cent) under CP100. According to the deterministic results, agricultural income is projected to increase across all EU Member States under carbon pricing. This result is driven by a combination of factors. First, because food demand in the EU exhibits relatively low price elasticities, a substantial share of the carbon cost is passed on to consumers through higher output prices. Second, under the assumed grandfathering scheme, producers can benefit from reducing emissions below their allocated permits and selling unused allowances, generating additional income in the form of permit rents. Finally, income effects are reinforced by production adjustments toward less emission-intensive, more profitable activities. At a more disaggregated level (see Fig. 5), agricultural income increases across all EU member states, indicating a broadly positive impact on farm-level profitability despite the distributional effects on consumers.

4.2 Carbon price with yield uncertainty

Considering yield uncertainty adds valuable information to the picture described in the previous section. Figure 6 shows the cumulative distribution of the mitigated EU and world agricultural emissions under the two scenarios. In both scenarios, the deterministic values are very close to the medians of the cumulative distribution functions. However, the CV of mitigated emissions under the CP50 scenario is 3.7. In contrast, under CP100, the uncertainty is 1.8, indicating that the uncertainty surrounding the amount of mitigated emissions is lower at a higher carbon price.[10] These variations in uncertainty across carbon prices arise from disparities in methane emissions from enteric fermentation. The magnitude of emissions from enteric fermentation depends on the feed mix used. Higher carbon prices prompt a shift in the feed mix toward more industrial and imported feed and cereals, among which cereals are susceptible to weather uncertainty. In contrast, industrial and imported feed can serve as a buffer against elevated feed costs due to higher carbon prices and reduced yields resulting from extreme weather events. Conversely, at lower carbon prices, a greater proportion of the feed originates locally and is directly impacted by weather uncertainty, encompassing fodder maize, other arable land fodder and straw. However, the probability that the amount of mitigated emissions under both scenarios will be lower or higher than the deterministic result is 50 per cent, although the distributions are negatively skewed, that is have a slightly longer left tail. This can be interpreted as implying that, in a good year, the deviation of the level of mitigated emissions from the median value will be smaller than in a bad year, resulting in a slower increase in mitigated emissions compared with the more rapid decrease in a bad year. In other words, beyond expanding the scale of mitigation, higher carbon pricing acts as a stabilizing mechanism by reducing the volatility of abatement outcomes. As prices rise, a structural transition from weather-dependent local fodder to standardized industrial feeds decouples methane emissions from climatic stochasticity.

Similar to the deterministic results, the stochastic results also show declining global agricultural GHG emissions, ranging from 3 to 6.8 Mt CO_2eq (CP50) and from 13.5 to 17.1 Mt CO_2eq (CP100). This means that under the CP50 scenario, from 62.9 to 80.2 per cent of the mitigated emissions in the EU will leak to non-EU countries. Under the CP100 scenario, from 49.8 to 57.2 per cent of the mitigated emissions in the EU will leak to non-EU countries. Interestingly, we again notice that the uncertainty around the leaked emissions from the EU to non-EU countries is lower under the 100€/tCO_2eq carbon price with a CV of 3.13 compared to the CV of 5.45 under the 50€/tCO_2eq.

Another significant source of uncertainty surrounding mitigated emissions is nutrient uptake[11] by crops (absorption), which is based on actual crop yields

10 Additional simulations for carbon prices of 75 and 125€/tCO_2eq yield coefficients of variation of 1.5 and 0.9, respectively, confirming that uncertainty is substantially lower at moderate-to-high carbon prices compared with CP50.

11 Nutrient uptake in CAPRI is influenced by three factors: crop-specific nutrient uptake factors (measured) in kg per t of yield, which when multiplied by the crop yields, yield the value of nutrient uptake per ha. By subsequently multiplying the calculated nutrient uptake per ha by the activity levels, we obtain the total nutrient uptake.

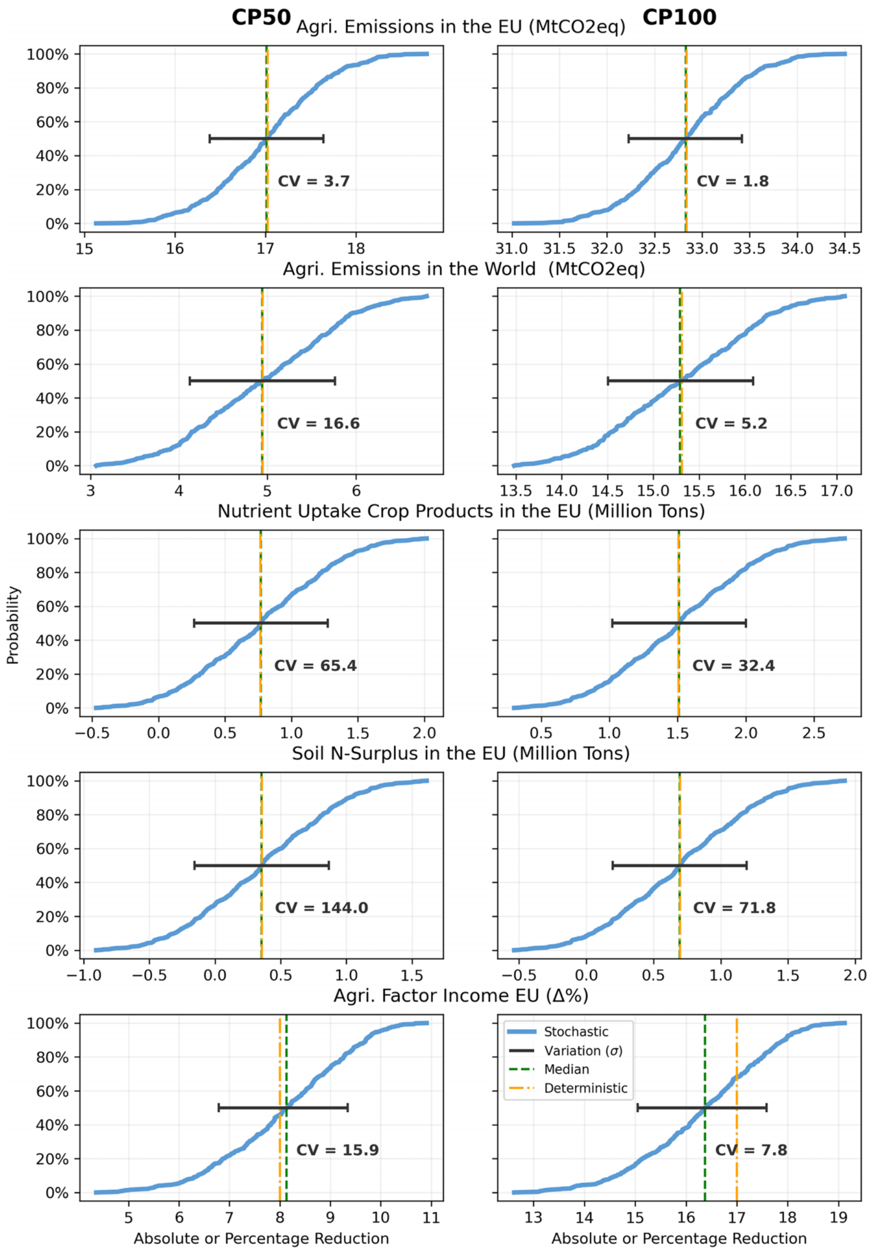

Fig. 6. Cumulative distribution functions of model outcomes under CP50 and CP100 scenarios, relative to the reference case.

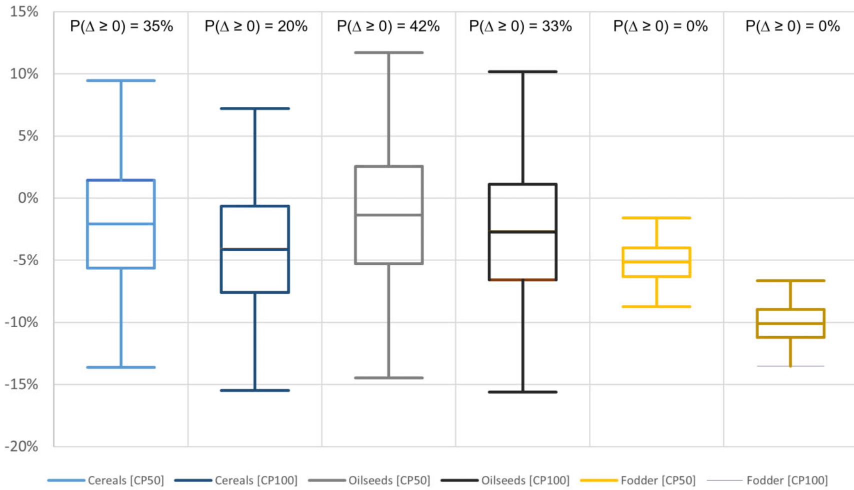

Fig. 7. Variation in EU agricultural supply compared to the reference scenario with consideration of yield uncertainty. A box and whisker plot shows the distribution of supply values, with the central box covering the 25th–75th quantiles, whiskers indicating extreme values, and a central line representing the median.

in a given year. These values are shown in Fig. 6. It can be seen that a carbon price of 50€/tCO_2eq in the deterministic setting already reduces the nutrient uptake by 0.77 MtCO_2eq compared with the reference scenario without a carbon price. However, when weather uncertainty is taken into account, there remains a 9 per cent probability that this value will not decrease. In contrast, with a carbon price of 100€/tCO_2eq, the likelihood of a decrease in nutrient uptake is higher, even with the consideration of weather uncertainty.

Changes in nutrient uptake levels drive changes in the N surplus at the soil level, resulting in higher leaching and runoff, denitrification and accumulation levels (Fig. 6). Nevertheless, it is worth noting that, when carbon pricing scenarios are considered without weather uncertainty, nutrient uptake by crops decreases as a result of changes in activity levels. Consequently, this reduction does not lead to an increase in the N surplus at the soil level. This, however, is not the case when changes in nutrient uptake are driven by weather uncertainty, as farmers have no flexibility to adjust fertilization levels. In this situation, a bad year (lower yields) increases, while a good year (higher yields) decreases the N surplus at the soil level. Under the CP50 scenario, there remains a 28 per cent probability that the N surplus increases as a result of extreme weather conditions compared with the reference scenario without carbon prices. Under the CP100 scenario, this probability falls to 10 per cent.

Although the deterministic results indicate that the production of cereals and oilseeds in the EU declines under the simulated scenarios, considering weather variability (Fig. 7) shows that, under the CP50 scenario, there

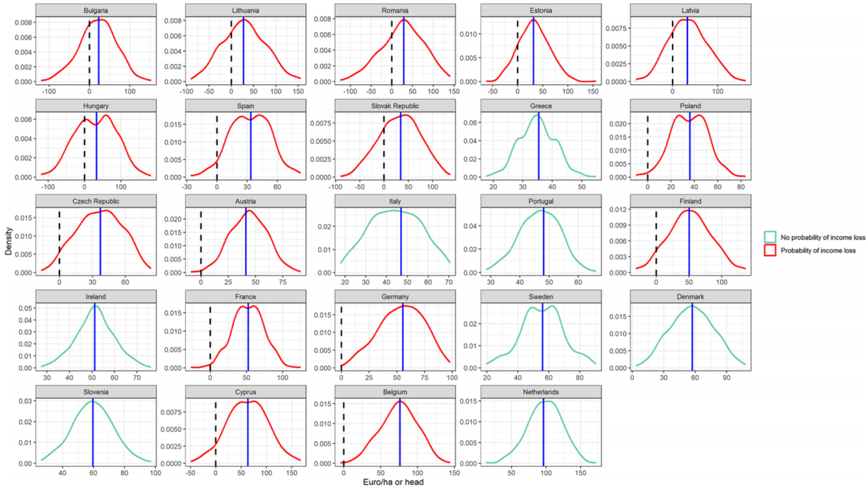

Fig. 8. Probability density functions of absolute changes in agricultural income (€/ha) in member states under a 50€/tCO_2eq carbon price compared to the reference scenario in 2030 (deterministic result shown as vertical line).

is a 35 and 42 per cent probability that cereal and oilseed production in the EU will not decrease relative to the reference scenario. Under the CP100 scenario, these probabilities fall to 20 and 33 per cent for cereal and oilseed production, respectively. Under both scenarios, fodder production is very likely to decrease. Since animal-producing activities are only indirectly affected by weather variability, there is only minor uncertainty surrounding the production of these commodities.

As shown in Fig. 6, under both scenarios, agricultural income in the EU continues to increase relative to the reference scenario. The income change ranges from 4 to 11 per cent under the CP50 and from 13 to 19 per cent under the CP100 scenarios. Nevertheless, when weather uncertainty is accounted for, there is, under both scenarios, a 54 per cent probability that the income change is lower than that implied by the deterministic point estimates.

However, at the member state level, some countries face the risk of reduced agricultural income. Under the CP50 scenario, sixteen member states exhibit varying probabilities of income reduction (Fig. 8). Bulgaria and Hungary face the highest risk, with a 32 per cent probability, followed by Romania and Lithuania at 29 and 28 per cent, respectively. Notably, countries with a substantial share of crop production are more vulnerable to income reductions due to weather variability. Under the CP100 scenario, the number of member states, as well as the risk of income reduction in these member states, decreases. In this case, only seven member states exhibit a probability of reduced income. Among these countries, Bulgaria, Romania and Hungary remain the most vulnerable, with probabilities of 19, 16 and 15 per cent, respectively (Fig. 9).

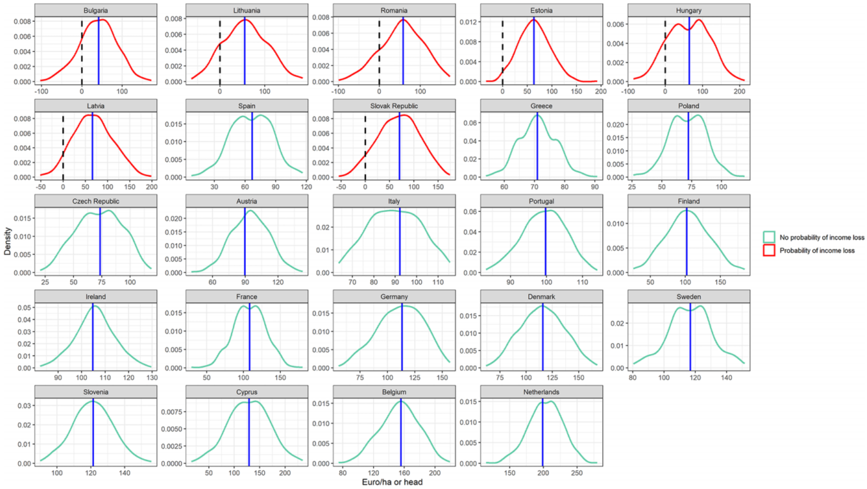

Fig. 9. Probability density functions of absolute changes in agricultural income (€/ha) in member states under a 100€/tCO_2eq carbon price compared to the reference scenario in 2030 (deterministic result shown as vertical line).

5. Discussion and conclusions

This article analyzes the impacts of carbon pricing on the EU agricultural sector, incorporating weather variability through simulations using the CAPRI model. It is essential to distinguish between the nature of the two shocks considered: carbon pricing represents a long-term economic shock, allowing farmers sufficient time to adjust their production decisions; in contrast, weather-related shocks, such as those affecting crop yields, occur during specific phenological stages, at which point adjustments to production patterns are no longer feasible. To capture the combined effects of these distinct shocks within a single simulation framework, we introduce a novel modeling approach within the CAPRI system, called IRGQ, which provides a high degree of approximation precision while requiring minimal computational capacity. This method is applicable beyond the CAPRI model and can be easily used with other modeling platforms. By integrating these features, the CAPRI framework evolves from being purely deterministic to incorporating stochastic elements. We argue that this methodological consideration is critical yet frequently overlooked in existing studies on climate policy instruments.

Our findings reveal several essential insights that have been overlooked in previous deterministic analyses of climate policy instruments (such as carbon pricing), including studies that do not account for the short-term nature of weather-induced yield variability when assessing these policies. First, the results demonstrate an inverse relationship between the carbon price and the uncertainty surrounding the volume of mitigated emissions. This pattern is not strictly monotonic across all carbon price levels; however, once carbon prices reach moderate levels (75€/tCO_2eq and above), the CVs of mitigated emissions remain consistently lower than under low-price scenarios. This variation in uncertainty is primarily driven by changes in the feed mix composition across different carbon pricing scenarios. Specifically, higher carbon prices prompt a shift toward greater reliance on industrially produced and imported feed and cereals, which are less sensitive to local weather variability and help stabilize feed costs during years of poor yields. In contrast, lower carbon prices encourage the use of locally produced feed sources, such as fodder maize and straw, which are more vulnerable to weather-related shocks. This reliance on weather-sensitive inputs amplifies the variability in emissions outcomes.

Second, our results suggest a significant risk of emissions leakage in the agricultural sector under both carbon pricing scenarios. Notably, the analysis points to a possible logarithmic relationship between the carbon price and the rate of emissions leakage, indicating that while leakage increases with higher carbon prices, the rate of increase diminishes. This implies a tapering effect, whereby the marginal impact of each additional unit of the carbon price becomes smaller. Furthermore, our findings are consistent with prior studies (e.g. Himics *et al.*, 2018; Jansson and Säll, 2018; Frank *et al.*, 2021), which identify the livestock sector, particularly meat production, as the primary contributor to total emissions leakage.

An important caveat to the interpretation of these leakage results is that they are derived under the assumption of unilateral EU climate action. The model does not account for the possibility that non-EU trading partners may implement or strengthen their own GHG mitigation policies in response to EU carbon pricing, nor does it represent coordinated international climate action. As a result, the estimated magnitude of emissions leakage should be interpreted as conditional on the absence of comparable mitigation efforts outside the EU and may therefore overstate long-run leakage under scenarios of increasing global climate policy alignment. Within this context, our results highlight the potential leakage pressures faced by the EU agricultural sector under unilateral carbon pricing, rather than providing a definitive assessment of leakage under globally coordinated climate action.

Important insights on the supply side also emerge that are not captured by the deterministic model. While deterministic simulations project a decline in the production of major crops in the EU as a consequence of carbon pricing, the stochastic model reveals a considerable probability that production levels may not only remain stable but also increase relative to the reference scenario. Another critical dimension uniquely captured by the stochastic framework concerns agricultural income at the member state level. The increase in agricultural income under carbon pricing observed in the deterministic results is the outcome of several reinforcing mechanisms. First, low price elasticities of food demand in the EU allow producers to pass a substantial share of carbon-related cost increases on to consumers. Second, as explained in Section 3, the assumed grandfathering of emission permits generates scarcity rents for producers: farmers who reduce emissions below their allocated permits can sell unused allowances at the prevailing carbon price, effectively receiving an implicit subsidy. These effects are further supported by production adjustments toward less emission-intensive activities. Taken together, these mechanisms explain the aggregate-level income gains.

Importantly, this result is conditional on the assumed policy design and demand characteristics and should not be interpreted as a general outcome of carbon pricing in agriculture. However, the stochastic model introduces an important nuance: member states that rely heavily on crop production face a significant risk of income loss from extreme weather events. These adverse outcomes are not apparent in deterministic analyses. Although the partial equilibrium nature of the CAPRI model does not allow for the modeling of potential redistribution mechanisms to compensate adversely affected consumers or producers, the incorporation of weather variability into the modeling framework highlights these vulnerabilities and underscores the importance of complementary policy interventions.

Additionally, integrating stochastic elements into the CAPRI model enables a more comprehensive assessment of policy impacts on the EU agricultural sector by accounting for the inherent uncertainty in factors such as weather variability and yield fluctuations. This enhancement is particularly significant for policy advice, given CAPRI's role as one of the principal simulation tools employed at the EU level. By reflecting a more realistic range of potential outcomes, the model can offer policymakers more robust and nuanced guidance.

As this is the first study to incorporate weather variability into the CAPRI model, several methodological limitations warrant further exploration. In the current analysis, yield uncertainty is modeled based on variability in national average yields. However, yield variability, and thus uncertainty faced by farmers, is typically more pronounced at the local level. Accounting for this spatial granularity would, however, exponentially increase the model's computational burden, as the number of stochastic variables would rise substantially. Moreover, this study does not account for yield uncertainty in non-EU regions or for other potential sources of uncertainty, such as market volatility or policy shifts.

Additionally, technical mitigation options are not included in the current modeling framework, as the focus is on evaluating the direct effects of weather-induced yield uncertainty on carbon pricing. Nevertheless, it is plausible that the inclusion of such technologies, whose adoption could be influenced by varying carbon price levels, would affect mitigation outcomes and potentially reduce result uncertainty. These technologies have direct implications for emissions reductions, productivity, input use and production costs.

Although the IRGQ method used in this study is efficient and thus suitable for CAPRI, the points generated by this method are restricted in their variation around the mean on each coordinate axis, which limits their ability to capture the extreme tails (i.e. rare occurrences) of the given probability distribution (Villoria and Preckel, 2017). This limitation has both drawbacks and benefits. While IRGQ cannot represent distributional tails and is therefore unsuitable for analyzing rare extreme events, many simulation models also perform poorly under large shocks, as such scenarios push them beyond their calibration range and undermine the empirical validity of their parameters (Stepanyan *et al.*, 2022). A second limitation of IRGQ is that the method is restricted to approximating symmetric distributions. Allowing for non-normal yield distributions would require Monte Carlo-based sampling to adequately capture higher-order moments, typically involving tens of thousands of model runs. Given the dimensionality of the stochastic system and the computational complexity of CAPRI, such an approach is not feasible in the present framework. Finally, the assumed interest rate of 1.9 per cent affects the results only through the calculation of the future value of the carbon price. As CAPRI is a PE model of the agricultural sector, it does not capture broader macroeconomic effects of alternative discount rates. Higher rates would therefore mainly scale the magnitude of the impacts without changing the qualitative results.

Acknowledgements

The authors thank the three anonymous reviewers for their valuable comments and suggestions, which have significantly improved the quality and clarity of this paper, and Ekaterina Iovleva for her valuable input throughout its preparation.

Author contributions

D. Stepanyan: Conceptualization; Methodology; Software; Formal Analysis; Writing – Original Draft. S. Neuenfeldt: Software; Formal Analysis; Writing – Review & Editing. A. Spiegel: Writing – Review & Editing. M. Söder: Writing – Review & Editing. J. Fournier Gabela: Writing – Review & Editing. F. Freund: Writing – Review & Editing. C. Heidecke: Writing – Review & Editing. B. Osterburg: Writing – Review & Editing. A. Gocht: Software; Formal Analysis; Writing – Review & Editing; Supervision.

Supplementary data

Supplementary data are available at *ERAE* online.

Conflicts of interest. None declared.

Funding

This research has been funded by the long-term climate mitigation policies for the agrifood sector (AGRILOP) project, financed by the Johann Heinrich von Thünen Institute in Braunschweig, Germany, from its own research budget. It was partially funded by the European Union Horizon Europe Grant Agreement No. 101134874: advancing capacity and analytic tools for supporting Common Agricultural Policies post 2027.

References

Araujo-Enciso, S. R., Pieralli, S., and Pérez-Domínguez, I. (2017). *Partial Stochastic Analysis with the Aglink-Cosimo Model: A Methodological Overview*. *JRC Technical Reports*. European Commission. https://doi.org/10.2760/680976

Arndt, C. (1996). 'An Introduction to Systematic Sensitivity Analysis via Gaussian Quadrature', *GTAP Technical Paper*. https://docs.lib.purdue.edu/cgi/viewcontent.cgi?referer=&httpsredir=1&article=1002&context=gtaptp. Date accessed 30 July 2023.

Arndt, C., and Hertel, T. W. (1997). 'Revisiting "The Fallacy of Free Trade"', *Review of International Economics*, 5: 221–9. https://doi.org/10.1111/1467-9396.00052

Batra, R. (1992). 'The Fallacy of Free Trade', *Review of International Economics*, 1: 19–31. https://doi.org/10.1111/j.1467-9396.1992.tb00004.x

BMEL (2018). 'Ernteberich 2018—Mengen und Preise', https://www.bmel.de/SharedDocs/Downloads/DE/_Landwirtschaft/Pflanzenbau/Ernte-Bericht/ernte-2018.html. Date accessed 8 July 2022.

Böhringer, C., Carbone, J. C., and Rutherford, T. F. (2012). 'Unilateral Climate Policy Design: Efficiency and Equity Implications of Alternative Instruments to Reduce Carbon Leakage', *Energy Economics*, 34: S208–17. https://doi.org/10.1016/j.eneco.2012.09.011

Britz, W. (2022). 'Implementing an Approximation of Cumulative Prospect Theory into Mixed Linear Programming—An Application to Bio-Economic Modelling at Farm-Scale Considering Crop Insurance', *German Journal of Agricultural Economics*, 71: 184–203. https://doi.org/10.30430/gjae.2022.0244

Burrell, A., and Nii-Naate, Z. (2013). *Partial Stochastic Analysis with the European Commission's Version of the AGLINK-COSIMO Model. JRC Reference Reports*. European Commission. https://data.europa.eu/doi/10.2791/87727. Date accessed 8 July 2022.

Ciais, P. et al. (2005). 'Europe-Wide Reduction in Primary Productivity Caused by the Heat and Drought in 2003', *Nature*, 437: 529–33. https://doi.org/10.1038/nature03972

Chatzopoulos, T. et al. (2021). 'Potential Impacts of Concurrent and Recurrent Climate Extremes on the Global Food System by 2030', *Environmental Research Letters*, 16: 124021. https://doi.org/10.1088/1748-9326/ac343b

EEA (2021). 'Annual European Union Greenhouse Gas Inventory 1990–2019 and Inventory Report 2021', *Submission to the UNFCCC Secretariat*, EEA/PUBL/2021/066. Brussels. https://www.eea.europa.eu/publications/annual-european-union-greenhouse-gas-inventory-2021. Date accessed 10 October 2023.

Ermolieva, T. et al. (2016). 'Integrated Management of Land Use Systems under Systemic Risks and Security Targets: A Stochastic Global Biosphere Management Model', *Journal of Agricultural Economics*, 67: 584–601. https://doi.org/10.1111/1477-9552.12173

ESABCC (2024). *Towards EU Climate Neutrality: Progress, Policy Gaps and Opportunities: Assessment Report 2024*. Publications Office of the European Union. https://data.europa.eu/doi/10.2800/73564. Date accessed 13 March 2025.

FAOSTAT (2022). *FAOSTAT Statistical Database*. Rome: Food and Agriculture Organization of the United Nations. https://www.fao.org/faostat/en/#compare. Date accessed 18 June 2023.

Fellmann, T. et al. (2018). 'Major Challenges of Integrating Agriculture into Climate Change Mitigation Policy Frameworks. Mitigation and Adaptation Strategies for Global Change', *Mitigation and Adaptation Strategies for Global Change*. 23: 451–68. https://doi.org/10.1007/s11027-017-9743-2

Frank, S. et al. (2019). 'Agricultural Non-CO2 Emission Reduction Potential in the Context of the 1.5°C Target', *Nature Climate Change*, 9: 66–72. https://doi.org/10.1038/s41558-018-0358-8

Frank, S. et al. (2021). ‘How Much Multilateralism Do We Need? Effectiveness of Unilateral Agricultural Mitigation Efforts in the Global Context’, *Environmental Research Letters*, 16: 104038. http://dx.doi.org/10.1088/1748-9326/ac2967

Fuss, S. et al. (2015). ‘Global Food Security & Adaptation Under Crop Yield Volatility’, *Technological Forecasting and Social Change*, 98: 223–33. https://doi.org/10.1016/j.techfore.2015.03.019

Glauber, J. W., and Westhoff, P. (2015). ‘The 2014 Farm Bill and the WTO’, *American Journal of Agricultural Economics*, 97: 1287–97. https://doi.org/10.1093/ajae/aav023

Gocht, A., and Witzke, P. (2024). ‘CAPRI’, https://www.capri-model.org/. Date accessed 20 November 2024.

Gocht, A. et al. (2017). ‘EU-Wide Economic and Environmental Impacts of CAP Greening with High Spatial and Farm-Type Detail’, *Journal of Agricultural Economics*, 68: 651–81. https://doi.org/10.1111/1477-9552.12217

Hasegawa, T. et al. (2018). ‘Risk of Increased Food Insecurity Under Stringent Global Climate Change Mitigation Policy’, *Nature Climate Change*, 8: 699–703. https://doi.org/10.1038/s41558-018-0230-x

Himics, M., Fellmann, T., and Barreiro-Hurle, J. (2020). ‘Setting Climate Action as the Priority for the Common Agricultural Policy: A Simulation Experiment’, *Journal of Agricultural Economics*, 71: 50–69. https://doi.org/10.1111/1477-9552.12339

Himics, M. et al. (2018). ‘Does the Current Trade Liberalization Agenda Contribute to Greenhouse Gas Emission Mitigation in Agriculture?’ *Food Policy*, 76: 120–9. https://doi.org/10.1016/j.foodpol.2018.01.011

IPCC (2006). ‘2006 IPCC Guidelines for National Greenhouse Gas Inventories’, in H.S. Eggleston, L. Buendia, K. Miwa, T. Ngara, and K. Tanabe (eds.) *Prepared by the National Greenhouse Gas Inventories Programme*, Japan: IGES. https://www.ipcc-nggip.iges.or.jp/public/2006gl/index.html. Date accessed 8 July 2023.

Jansson, T., and Säll, S. (2018). ‘Environmental Consumption Taxes on Animal Food Products to Mitigate Greenhouse Gas Emissions from the European Union’, *Climate Change Economics*, 9: 1850009. https://doi.org/10.1142/S2010007818500094

Jansson, T. et al. (2020). ‘Coupled Agricultural Subsidies in the EU Undermine Climate Efforts’, *Applied Economic Perspectives and Policy*, 43: 1503–19. https://doi.org/10.1002/aepp.13092

Jongeneel, R., and Gonzalez-Martinez, A. R. (2020). ‘Estimating Crop Yield Supply Responses to Be Used for Market Outlook Models: Application to Major Developed and Developing Countries’, *NJAS: Wageningen Journal of Life Sciences*, 92: 1–13. https://doi.org/10.1016/j.njas.2020.100327

Leip, A. et al. (2010). *Evaluation of the Livestock Sector’s Contribution to the EU Greenhouse Gas Emissions (GGELS)—Final Report*. European Commission, Joint Research Centre. https://op.europa.eu/en/publication-detail/-/publication/38abd8e0-9fe1-4870-81da-2455f9fd75ad. Date accessed 30 March 2023.

Lobell, D. B., Baldos, U. L. C., and Hertel, T. W. (2013). ‘Climate Adaptation as Mitigation: The Case of Agricultural Investments’, *Environmental Research Letters*, 8: 015012. https://doi.org/10.1088/1748-9326/8/1/015012

Meyer, S., Binfield, J., and Westhoff, P. (2012). ‘Technology Adoption Under US Biofuel Policies: Do Producers, Consumers or Taxpayers Benefit?’ *European Review of Agricultural Economics*, 39: 115–36. https://doi.org/10.1093/erae/jbr045

OECD/FAO (2015). ‘Aglink-Cosimo Model Documentation’, *A Partial Equilibrium Model of World Agricultural Markets*. http://www.agri-outlook.org/about/Aglink-Cosimo-model-documentation-2015.pdf. Date accessed 1 April 2023.

Pérez Domínguez, I. (2005). *Greenhouse Gases: Inventories, Abatement Costs and Markets for Emission Permits in European Agriculture: A Modelling Approach*. *Dissertation*. Bonn: Rheinische Friedrich-Wilhelms-Universität Bonn. https://nbn-resolving.org/urn:nbn:de:hbz:5N-05383. Date accessed 30 March 2023.

Pérez Domínguez, I. et al. (2020). 'Economic assessment of GHG mitigation policy options for EU agriculture: A closer look at mitigation options and regionalmitigation costs - EcAMPA 3. Edited by Thomas Fellmann', *JRC Science for Policy Report*. Publications Office of the European Union. https ://data.europa.eu/doi/10.2760/552529.

Saltelli, A. et al. (2020). 'Five Ways to Ensure That Models Serve Society: A Manifesto', *Nature*, 582: 482–4. https://doi.org/10.1038/d41586-020-01812-9

Sørensen, P. B. et al. (2025). 'The Effects of Unilateral Climate Policy Towards Agriculture: A Case Study of Denmark', *Journal of Agricultural Economics*, 76: 3–23. https://doi.org/10.1111/1477-9552.12624

Stepanyan, D., Zimmermann, G., and Grethe, H. (2022). 'Stochastic Simulation with Informed Rotations of Gaussian Quadratures', *Economic Systems Research*, 35: 30–48. https://doi.org/10.1080/09535314.2022.2045258

Stepanyan, D. et al. (2021). 'Multiple Rotations of Gaussian Quadratures: An Efficient Method for Uncertainty Analyses in Large-Scale Simulation Models', *Environmental Modelling & Software*, 136: 104929. https://doi.org/10.1016/j.envsoft.2020.104929

Stepanyan, D. et al. (2023). 'Impacts of National vs European Carbon Pricing on Agriculture', *Environmental Research Letters*, 18: 074016. https://doi.org/10.1088/1748-9326/acdcac

Stroud, A. H. (1957). 'Remarks on the Disposition of Points in Numerical Integration Formulas', *Mathematical Tables and Other Aids to Computation*, 11: 257–61. https://doi.org/10.2307/2001945

Valenzuela, E. et al. (2007). 'Assessing Global Computable General Equilibrium Model Validity Using Agricultural Price Volatility', *American Journal of Agricultural Economics*, 89: 383–97. https://doi.org/10.1111/j.1467-8276.2007.00977.x

Valin, H. et al. (2015). *The Land Use Change Impact of Biofuels Consumed in the EU: Quantification of Area and Greenhouse Gas Impacts*. Netherlands: Utrecht. http://pure.iiasa.ac.at/id/eprint/12310/.

van Meijl, H. et al. (2018). 'Comparing Impacts of Climate Change and Mitigation on Global Agriculture by 2050', *Environmental Research Letters*, 13: 064021. https://doi.org/10.1088/1748-9326/aabdc4

Verma, M., Hertel, T. W., and Valenzuela, E. (2011). 'Are The Poverty Effects of Trade Policies Invisible?' *The World Bank Economic Review*, 25: 190–211. https://doi.org/10.1093/wber/lhr014

Villoria, N. B. et al. (2013). 'Will Yield Improvements on the Forest Frontier Reduce Greenhouse Gas Emissions? A Global Analysis of Oil Palm', *American Journal of Agricultural Economics*, 95: 1301–8. https://doi.org/10.1093/ajae/aat034

Villoria, N. B., and Mghenyi, E. W. (2017). 'The Impacts of India's Food Security Policies on South Asian Wheat and Rice Markets', *The World Bank Economic Review*, 31: 730–46. https://doi.org/10.1093/wber/lhw002.

Villoria, N. B., and Preckel, P. V. (2017). 'Gaussian Quadratures vs. Monte Carlo Experiments for Systematic Sensitivity Analysis of Computable General Equilibrium Model Results', *Economics Bulleltin*, 37: 480–7. http://www.accessecon.com/Pubs/EB/2017/Volume37/EB-17-V37-I1-P43.pdf. Date accessed 30 July 2023.

Webber, H. et al. (2020). 'No Perfect Storm for Crop Yield Failure in Germany', *Environmental Research Letters*, 15: 104012. https://doi.org/10.1088/1748-9326/aba2a4

Westhoff, P. C., Brown, S., and Hart, C. (2006). 'When Point Estimates Miss the Point: Stochastic Modeling of WTO Restrictions', *Journal of International Agricultural Trade and Development*, 2: 79–85. https://ageconsearch.umn.edu/record/49155?ln=en&v=pdf. Date accessed 30 July 2023.
World Bank (2021). *State and Trends of Carbon Pricing 2021*. Washington, DC: World Bank. https://doi.org/10.1596/978-1-4648-1728-1

Appendix 1

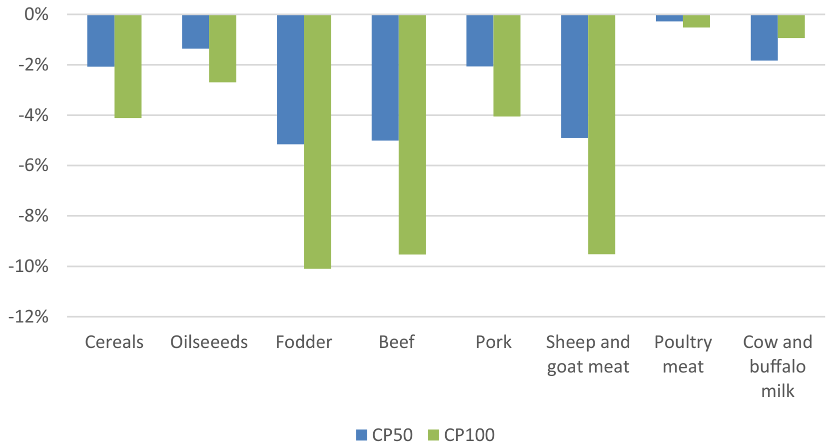

Fig. A1. Percentage change in the EU agricultural supply compared to the reference scenario.

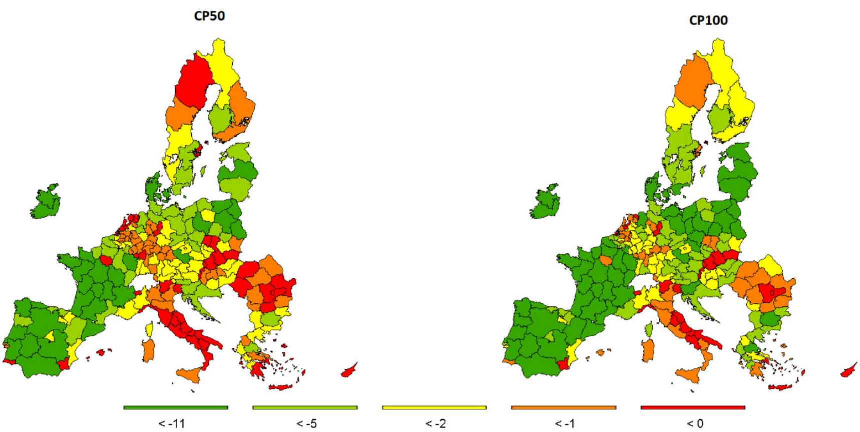

Fig. A2. Absolute changes in beef cattle herd size in 1,000 heads compared to the reference scenario.

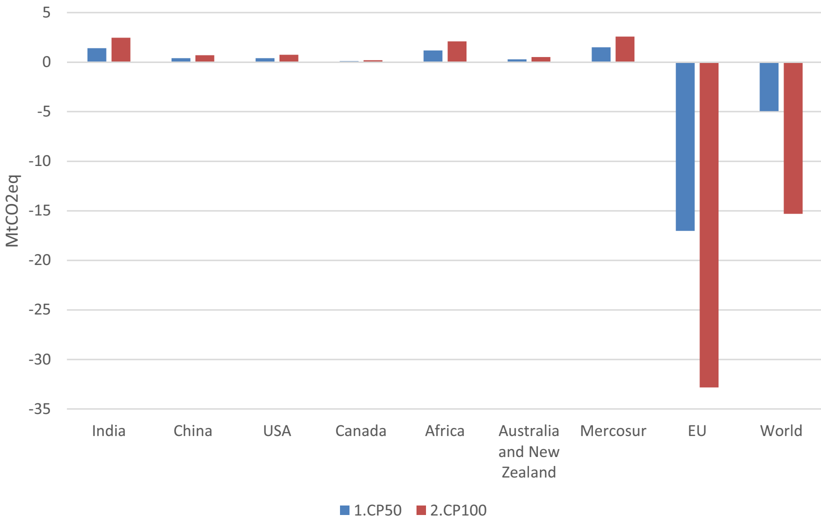

Fig. A3. Leakage of agricultural emissions by 2030 compared to the reference scenario, in absolute terms.

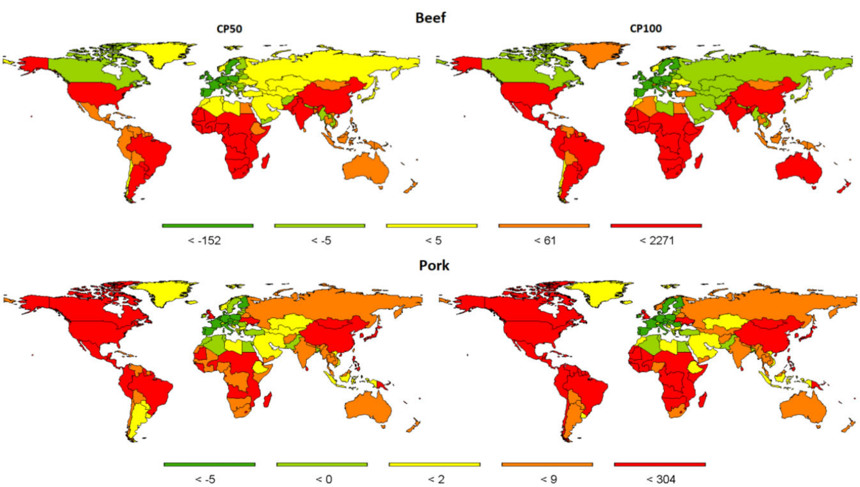

Fig. A4. Absolute differences in beef and pork production-induced emission leakage by 2030 [1,000 t CO_2eq] compared to the reference scenario.

Table A1. Country-crop combinations treated as stochastic in the model and whether the original deviations are normally distributed (N) or have been transformed (T) to achieve normality.

	Belgium	Sweden	Denmark	Germany	Greece	Spain	France	Ireland	Italy	Netherlands	Austria	Portugal	Cyprus	Estonia	Latvia	Lithuania	Poland	Slovakia	Bulgaria	Czechia	Hungary	Slovenia	Romania	Finland
Soft wheat	N	N	N	N	**T**	N	N	N	N	N	N	N		N	N	**T**	N	N	**T**	N	N	N	N	
Durum wheat				N	**T**	**T**	N		N		N	N	N					N					N	
Barley	N	N	N	N	N	N	**T**	N	N	N	N	N	N	N	N	**T**	N	N	N	N	N	N	N	**T**
Fodder maize	N		N	**T**		N	N	N	N	N	N	N		N	N	N	**T**	**T**	N	N	N		N	
Maize	N			N		N	N		**T**	N	N	**T**					**T**	N	N	N	**T**	N	N	
Oats		N		N	N	N	N		N		N	N	N	N	N		**T**		N	N	N		N	**T**
Other cereals	N	N		N	N	N	N		N		N	N		N	N		N			N			N	
Other fodder on arable land	N	N	N	N	N	N	N	N	N	N	N	N	N	N	N	N	**T**	N	N	N	N	N	N	**T**
Potatoes	N	N	N	N	N	N	N	N		N	N	N	N	N	N		N	N	N	N	N		N	
Pulses	N	N	N	N			N	N		N	N	N	N	N	N	N	N	N		N	N	N	N	N
Rapeseed	N	N	N	N		N	N		N	N	N				N	N	N	N	N	**T**	N	N		
Fodder root crops	N		N		N				N	N			N	N	N	N	N			N	N		N	
Rye and meslin	N	N	N	N		N	N	N			N	N		N	N	N	N		N		N	N	N	
Sugar beet		N		N	N	N	**T**			N	N	N				N	N			N	N			N
Sunflower				N	N	N	N		**T**		N	N						N	N	N	N	N	**T**	

Note: **N** indicates that the deviations from the cubic trend are normally distributed according to the Shapiro–Wilk test for normality at the 5 per cent significance level. **T** indicates that the deviations from the cubic trend are not normally distributed; therefore, deviations from a linear trend that are normally distributed according to the Shapiro–Wilk test at the 5 per cent significance level are used instead (17 cases out of 253). Empty cells indicate that either the crop is not grown in the country or its share is not significant; therefore, it has not been selected.

Table A2. Sources and remains of nitrate used in Eu agriculture.

		Value in Baseline		CP50				CP100			
		Total	Per ha	Total		Per ha		Total		Per ha	
		(in 1,000 t)	(in kg)	Abs. change (in 1,000 t)	Per cent change	Abs. change (in kg)	Per cent change	Abs. change (in 1,000 t)	Per cent change	Abs. change (in kg)	Per cent change
Source	Mineral fertilizer	9,888.06	61.76	−474.75	−4.80%	−2.6	−4.21%	−925.47	−9.36%	−5.05	−8.18%
	Manure	7,973.12	49.8	−268.92	−3.37%	−1.38	−2.78%	−520.34	−6.53%	−2.64	−5.31%
	Crop residues	8,492.95	53.05	−427.23	−5.03%	−2.36	−4.44%	−839.4	−9.88%	−4.62	−8.71%
	Biological fixation	1,603.16	10.01	−78.38	−4.89%	−0.43	−4.30%	−157.59	−9.83%	−0.87	−8.66%
	Atmospheric deposition	1,826.23	11.41	−11.47	−0.63%	0	−0.01%	−24.01	−1.31%	0	−0.03%
Remains	Absorption by crop	19,667.24	122.85	−767.25	−3.90%	−4.06	−3.31%	−1506.84	−7.66%	−7.94	−6.46%
	Surplus total	10,116.28	63.19	−493.5	−4.88%	−2.71	−4.29%	−959.97	−9.49%	−5.25	−8.31%
	Gaseous loss	2,859.37	17.87	−96.26	−3.37%	−0.49	−2.82%	−186.88	−6.54%	−0.95	−5.61%
	Runoff mineral	408.3	2.55	−19.21	−4.70%	−0.1	−4.12%	−37.34	−9.15%	−0.2	−7.96%
	Runoff manure	434.4	2.71	−13.53	−3.11%	−0.07	−2.51%	−26.14	−6.02%	−0.13	−4.80%
	Surplus at soil level	6,414.21	40.07	−364.5	−5.68%	−2.04	−5.10%	−709.61	−11.06%	−3.97	−9.91%

Appendix 2. IRGQ as an efficient method to simulate stochastic shocks

Let us consider the following problem of stochastic modeling. Given a model variable or parameter x, a probability density function $g(x)$ that represents the uncertainty around x, and a model function $f(x)$ for which the expected value is sought, the integration problem can be expressed as follows:

$$E\left[f\left(x\right)\right] = \int_a^b f\left(x\right) g\left(x\right) dx. \tag{A1}$$

Since these integrals typically do not have analytical solutions, they must be approximated numerically using the following finite sum:

$$\tilde{E}\left[f\left(x\right)\right] = \sum_{i=1}^{n} f\left(x_i\right) w_i, \tag{A2}$$

where x_i are the n points (nodes) chosen from the domain of integration, and w_i are the corresponding weights. Various methods exist for selecting these weights. However, given the large scale and detailed nature of the CAPRI model utilized in this study, along with its significant computational demands, the IRGQ method (Stepanyan *et al.*, 2022) was chosen for its ability to produce accurate approximations using the minimum number of points, i.e. $2n$ points.

The IRGQ method is based on the degree 3 quadrature formulae by Stroud (1957). For $k = 1, \ldots, 2n$, let $\Gamma_k(\gamma_{k,1}, \gamma_{k,2}, \ldots, \gamma_{k,n})$ be the kth quadrature point, where

$$\gamma_{k,2j-1} = \sqrt{\frac{2}{3}}\cos\left(\frac{\left(2j-1\right)k\pi}{n}\right), \tag{A3}$$

$$\gamma_{k,2j} = \sqrt{\frac{2}{3}}\sin\left(\frac{\left(2j-1\right)k\pi}{n}\right), \tag{A4}$$

for $j = 1, \ldots, (n/2)$, where $(n/2)$ is the greatest integer not exceeding $n/2$. If n is odd,

$$\gamma_{k,n} = \frac{\left(-1\right)^k}{\sqrt{3}}. \tag{A5}$$

Arndt (1996) adjusted Stroud's formulae for multivariate standard normal distributions over all of R^n (Euclidean space). For $k = 1, \ldots, 2n$, let $\Gamma_k(\gamma_{k,1}, \gamma_{k,2}, \ldots, \gamma_{k,n})$ be the kth quadrature point, where

$$\gamma_{k,2j-1} = \sqrt{2}\cos\left(\frac{\left(2j-1\right)k\pi}{n}\right), \tag{A6}$$

$$\gamma_{k,2j} = \sqrt{2}\sin\left(\frac{\left(2j-1\right)k\pi}{n}\right), \tag{A7}$$

for $j = 1, \ldots, (n/2)$, where $(n/2)$ is the greatest integer not exceeding $n/2$. If n is odd,

$$\gamma_{k,n} = \left(-1\right)^k. \tag{A8}$$

The detailed calculations explaining this transformation can be found in Stepanyan *et al.* (2021).

The final stochastic points ($\overrightarrow{GQ_k}$) are calculated as follows:

$$\overrightarrow{GQ_k} = A \cdot \overrightarrow{\Gamma}_k + \overrightarrow{\mu}, \tag{A9}$$

where $\overrightarrow{\mu}$ is the vector of mean values of the stochastic components; A is a square matrix satisfying $\Sigma = AA^T$. There are many different methods of extracting the square matrix A from the covariance matrix (Σ), in this paper, however, we use the diagonalization method also known as eigensystem decomposition.

Stepanyan *et al.* (2022) improved the method by proposing to select such GQ points that have the largest dispersion. The dispersion of the kth GQ family $\overrightarrow{GQ_k}$ is the minimum of the distances between any two nodes $\overrightarrow{x}_i, \overrightarrow{x}_j \overrightarrow{x}_j$ of the family, i.e.

$$\text{disp}\left(\overrightarrow{GQ_k}\right) = \min\left\{\|\overrightarrow{x}_i - \overrightarrow{x}_j\| : \overrightarrow{x}_i, \overrightarrow{x}_j \in \overrightarrow{GQ_k},\ i, j = 1, \ldots, 2n,\ i \neq j\right\}, \tag{A10}$$

where k is the index number of the evaluated GQ family, and $\| \cdot \|$ is the Euclidean norm of a vector. Thereafter, the GQ with the largest dispersion, i.e. $\max(\text{disp}(\overrightarrow{GQ_k}))$, is selected. They showed that it improves the quality of approximated results considerably requiring the minimum number of model solutions.